INSTITUTE FOR NUCLEAR STUDY
UNIVERSITY OF TOKYO
Tanashi, Tokyo 188
Japan

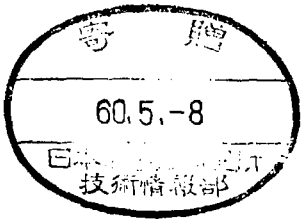

INS-Rep.-534
March 1985

The Origin of Nuclear Mass Number Dependence in EMC-Effect

INS 232,233 Collaboration

Y.Kurihara, S.Daté, A.Nakamura,

H.Sato, H.Sumiyoshi and K.Yoshinada

INS-Rep.-534
March 1985

The Origin of Nuclear Mass Number Dependence in EMC-Effect

INS 232,233 Collaboration
Y.Kurihara[1], S.Daté[2], A.Nakamura[3],
H.Sato, H.Sumiyoshi[4] and K.Yoshinada[5]
Institute for Nuclear Study, University of Tokyo,
Tanashi, Tokyo 188 JAPAN

Abstract:

The origin of the mass number dependence of the nucleon structure functions extracted from the deep inelastic lepton -nucleus scattering is investigated by factorizing the structure function into A and x dependent parts. It is found that the mass number dependence is determined by the probability of exotic components in multi-nucleon overlap. This suggests that the deformation of the nucleon structure function is caused by the interaction among nucleons during their overlap.

~~Present~~ Address after April 1.

1) Institut für Theoretische Physik, Univ. Tübingen, D-7400 Tübingen, West Germany
2) Dept. of Physics, Dalhousie Univ., Halifax, N.S., Canada
3) Institute für Theorie der Elementarteilchen, Freie Univ. Berlin, D-1000 Berlin, West Germany
4) Institute for Cosmic Ray Research, Univ. of Tokyo, Tokyo
5) Research Center of Ion Beam Technology, Hosei Univ., Tokyo

Since the European Muon Collaboration (EMC) suggested a significant difference between the nucleon structure functions extracted from muon-iron and muon-deuterium scattering experiments[1], many experimental and theoretical attempts have been undertaken to study this difference[2]. Recently, quite clear target mass number (A) dependence of the ratio of the nucleon structure function have been obtained by the deep inelastic electron-nucleus scattering experiment at SLAC[3]. Daté et al.[4] have investigated this A-dependence by factorizing the nucleon structure function into A and x dependent parts and found a new kind of scaling phenomenon and the existence of A-independent exotic components in the nucleon structure function. However their theoretical explanation on the A-dependence of the nucleon structure function was too naive to get the insight on the true nature of the exotic component. Therefore in this paper, firstly we investigate the origin of the A-dependence of the nucleon structure functions quantitatively by employing the realistic nuclear wave functions and try to answer the question "Where does the A independent exotic component in x part come from ?". Secondly we try to extract the absolute value of the probability of the exotic component in the nucleus from the SLAC data to compare it with the theoretical value calculated, while we still have some ambiguity due to the lack of information on the nucleon structure functions of neutron rich nuclei.

When the nucleons approach to one another, they

exchange gluons and quarks frequently, and hence the state other than the superposition of each nucleon is expected to be formed. We regard such an exotic state as the origin of abnormal A-dependence observed in deep inelastic lepton-nucleus scattering experiments. Thus in such a collision process of large four momentum transfer, the nuclear structure function per nucleon $F_2^A(x)$ is given by

$$F_2^A(x) = (1-P_{exo}^T(A))F_2^N(x) + P_{exo}^2(A)F_{exo}^2(x) + P_{exo}^3(A)F_{exo}^3(x) + \cdots, \quad (1)$$

where $P_{exo}^i(A)$ and $F_{exo}^i(x)$ are the probability and structure function for the exotic component in the i-body overlap. F_2^N is the structure function of the free nucleon. The total probability $P_{exo}^T(A)$ for finding exotic components is given by

$$P_{exo}^T(A) = \sum_{i=2}^{A} P_{exo}^i(A). \quad (2)$$

According to the non-relativistic quark Resonating Group Method calculation for the two-nucleon system[5], the realistic matter distribution is not so different from the nuclear distribution given by the orthodox nuclear physics. Therefore we assume that the normal two-nucleon component transforms into the two-body exotic one with the rate of $f_{exo}(r)$ at the relative distance r. Thus the average probability of the exotic component $\bar{p}(A)$ in each two-nucleon pair is defined by[6]

$$\bar{p}(A) = \frac{1}{\frac{1}{2}A(A-1)} \sum_{i<j} \langle \Psi_A | f_{exo}(r_{ij}) | \Psi_A \rangle. \quad (3)$$

With this $\bar{p}(A)$ value, the average probability $P_{exo}^2(A)$ of the two-body exotic component in the nucleus A is given by

$$P_{exo}^2(A) = (A-1)\,\bar{p}(A)\,\{1-\bar{p}(A)\}^{A-2}. \quad (4)$$

If $\bar{p}(A)$ is much smaller than unity, $P_{exo}^2(A)$ is approximately given by

$$P_{exo}^2(A) \simeq (A-1)\,\bar{p}(A). \quad (5)$$

Here we note that the neglection of the last term in the RHS of eq.(4) leads to the overestimation of the probability for exotic components. (Sometimes we find eq.(5) used with rather long-ranged $f_{exo}(r_{ij})$ which produces rather large values of $\bar{p}(A)$.)

The function $f_{exo}(r_{ij})$ is obtainable from the overlap of the quark density in the two-nucleon pair. Since the quark density distribution is possibly given by a gaussian form $\rho_0 \exp(-x^2/b^2)$, the $f_{exo}(r_{ij})$ may be defined by

$$f_{exo}(r_{ij}) = \int d\vec{x}\, \exp -(\vec{x}+\vec{r}_{ij}/2)^2/b^2 \, \exp -(\vec{x}-\vec{r}_{ij}/2)^2/b^2 \times \left[\int d\vec{x}\, \exp(-2x^2/b^2) \right]^{-1}$$

$$= \exp\left\{-r_{ij}^2/(2b^2)\right\}. \quad (6)$$

Here the size parameter b is usually taken as 0.5 to 0.6 fm.

We estimate the $P^2_{exo}(A)$ for three b values of 0.5, 0.55 and 0.6 fm by employing following wave functions: For ^{4}He, the one which takes account of the short-range correlation[7], realistic nuclear shell model wave functions for ^{9}Be to ^{27}Al[8], and simple Slater determinants of Woods-Saxon single particle wave functions for nuclei larger than ^{27}Al. The numerical values of $P^2_{exo}(A)$ obtained are tabulated in Table I. Although the absolute value of $P^2_{exo}(A)$ is sensitive to the choice of the value of b, its A-dependence is not so. For comparison, we also tabulate the sum of the probabilities of the i-body exotic components (i>2) $P^{i>2}_{exo}(A)$ in Table I, which is obtained by subtracting the $P^2_{exo}(A)$ from the sum of the probabilties of the i-body exotic components (i≥2) given by $1-\{1-p(A)\}^{A-1}$. As expected, $P^{i>2}_{exo}(A)$ is very small.

To see the spatial dependence of $P^2_{exo}(A)$, we examine the single particle state dependence of the $P^2_{exo}(A)$ in such a way that: Employing a Slater determinant of single particle wave functions, we can rewrite eq.(3) as follows,

$$\bar{p}(A) = \frac{1}{A}\sum_{\alpha} p_{\alpha}(A), \tag{7}$$

where

$$p_{\alpha}(A) = \frac{1}{2(A-1)}\sum_{\beta}\langle\phi_{\alpha}(1)\,\phi_{\beta}(2)\,|f_{exo}(r_{12})|\,\phi_{\alpha}(1)\,\phi_{\beta}(2)-\phi_{\alpha}(2)\,\phi_{\beta}(1)\rangle. \tag{8}$$

Here ϕ_{α} and ϕ_{β} are single particle wave functions having quantum numbers of α and β, respectively. The probability

$P^{2,\alpha}_{exo}(A)$ of the two-body exotic component for the nucleon in the single particle state α is defined by

$$P^{2,\alpha}_{exo}(A) = (A-1)\,p_{\alpha}(A)\,\{1-p_{\alpha}(A)\}^{A-2}. \tag{9}$$

The $P^{2,\alpha}_{exo}(A)$ for ^{40}Ca is tabulated in Table II. As seen in Table II, the probability $P^{2,\alpha}_{exo}(A)$ in the higher single nucleon state is not so small compared to those for the lower states. This indicates that the probability of the exotic component is almost independent of the spatial position of the nucleon, whether it stays inside or outside of the nucleus. This result is different from that intuitively obtained by Daté et al[4], who have treated the $P^2_{exo}(A)$ term as the single particle property in the nuclear distribution. On the other hand, since the $P^2_{exo}(A)$ term is treated as a realistic pairwise property in this work, its effect obtained is very similar to the pairing correlation in the nucleus and shows very small single particle state dependence.

Next we extract the corresponding experimental value of $P^2_{exo}(A)$ by employing the scaling assumption[4]. To extract the absolute values of $P^2_{exo}(A)$ from experimental data, we take account of the isospin dependent effects properly by introducing the following functions:

(i) The structure function of neutron is more rapidly damping with increasing x than that of proton. This effect

can be expressed as $f(x) \neq 0$, where

$$f(x) = (F_2^p(x) - F_2^n(x))/(F_2^p(x) + F_2^n(x)). \qquad (10)$$

(ii) Since the number of excess neutrons is defined for each nucleus A, we introduce the weight $Y(A)$ of neutron excess by

$$Y(A) = (N-Z)/A = 1 - 2Z/A, \qquad (11)$$

where Z and N are the proton and neutron number, respectively. The excess neutrons bring the additional A-dependence into the ratio $R_A(x)$ of the nucleon structure function and make a deviation in the $R_A(x)$ from unity near x=1 even if there exists no exotic component. Taking account of the above isospin dependent effects properly, we adjust the $P^2_{exo}(A)$ so as to fit the experimental $R_A(x)$*);

$$R_A(x) = \frac{\tilde{F}_2^A(x)}{\tilde{F}_2^d(x)}\left\{1-P^2_{exo}(A)\right\} + Q(x)\ P^2_{exo}(A), \qquad (12)$$

where $Q(x)$ is the ratio of the structure function of the exotic component to that of the free nucleon and is assumed to be A-independent. The structure functions of normal nucleon parts $\tilde{F}_2^A(x)$ and $\tilde{F}_2^d(x)$ are defined by

*) While the cross sections in Ref.3) were corrected so as to compensate for neutron excess, here we have pull back the data into the original ones.

$$\tilde{F}_2^A(x) = \frac{1}{A}\left\{Z\ F_2^p(x) + N\ F_2^n(x)\right\}, \qquad (13)$$

and

$$\tilde{F}_2^d(x) = \frac{1}{2}\left\{F_2^p(x) + F_2^n(x)\right\}. \qquad (14)$$

In other words the experimental probability, which should be compared with the theoretical one calculated before, can be obtained with the following formula by asking the self-consistency condition:

$$P^2_{exo}(A) = \left\{R_A(x)-1+Y(A)f(x)\right\} / \left\{Q(x)-1+Y(A)f(x)\right\}. \qquad (16)$$

Here we note following interesting consequences with eq.(16) : The $P^2_{exo}(A)$ extracted by Daté et al.[4] is corresponding to the case of $Y(A) = 0$ in eq.(16), where only the product of $P^2_{exo}(A)$ and $(Q(x)-1)$ can be determined from the experimental data. This is the reason why they could predict the A-dependence of $P^2_{exo}(A)$ well but could not determine the absolute value of $P^2_{exo}(A)$ solely. On the other hand, since the A-dependent term of $Y(A)f(x)$ appears in the denominator of eq.(16) in addition to the A-independent function of $(Q(x)-1)$, in principle, the absolute value of $P^2_{exo}(A)$ is obtainable with our treatment.

Employing the structure functions F_2^p and F_2^n obtained by Glück, Hoffmann and Reya[9] and parametrizing the A-independent function $Q(x)$ with a forth-order polynomial

$$Q(x) = \sum_{l=0}^{4} C_l x^l. \qquad (15)$$

We determine parameters $P^2_{exo}(A)$ and C_l in eq.(12) with the

least square fitting program SALS[10] from the experimental data $R_A(x)$ at $0.3 < x < 0.8$. The results are tabulated in Table III and IV. Here we perform the calculation in the following procedure : We first run the SALS with all $P^2_{exo}(A)$ and C_1 as free parametrs. However, since the absolute value of $Y(A)f(x)$ is very small, we find that it is rather difficult to determine the absolute values of $P^2_{exo}(A)$ without any ambiguity. Therefore as the second step, we fix the $P^2_{exo}(Al)$ to the mean value obtained in the first run and then repeat the same procedure. In this sense, we could so far only make a restriction on the absolute value of $P_{exo}(A)$ instead of the exact determination of the absolute value because of the smallness of the term of $Y(A)f(x)$. To determine $P^2_{exo}(A)$ and $Q(x)$ definitely, more experimental data of $R_A(x)$ especially for neutron rich nuclei are requested.

The values of $P^2_{exo}(A)$ derived from experimental data are tabulated in Table III. Table III shows that the $P^2_{exo}(A)$ strongly depends on the nuclear density distribution; for examples, $P^2_{exo}(^4He)$ is the almost same as $P^2_{exo}(^9Be)$ and $P^2_{exo}(A)$ are saturated for large nuclei, except ^{197}Au. To examine the consistency of our procedure, we calculate $R_A(x)$ employing the derived values of $P^2_{exo}(A)$ and $Q(x)$ and show the results in Fig.1. As seen in Fig.1, we confirm that the $Q(x)$-scaling suggested by Daté et al.[4] works very well.

The value of $P^2_{exo}(A)$ calculated with b= 0.55 fm is compared with the empirical $P^2_{exo}(A)$ in Fig.2. As seen in

Fig.2, the value of $P^2_{exo}(A)$ calculated nicely reproduces the A-dependence and the absolute value of the empirical $P^2_{exo}(A)$. Since the value of the size parameter b is chosen to be consistent with the non-relativistic quark shell model, this nice agreement between theoretical and experimental probabilties supports our original assumption that the exotic component is mainly produced by the two-nucleon overlap in a nucleus. Thus we conclude that the EMC-effect is due to the two-nucleon dynamics in a nucleus.

Here let us briefly compare our result with those obtained by other works. The work performed by Dias de Deus, Pimenta and Varela[11] corresponds to the case of no factorization and full exotics from our sense. On the other hand, Jaffe et al.[12] have tried to explain the SLAC data under the dynamical rescaling hypothesis by introducing the effective confinement size which is determined by the probability (P_{6q}) of finding the six-quark component in a nucleus. However to explain the data, they had to employ unbelievablly large amount of P_{6q}, for instance, 0.7 of P_{6q} for Au and Pb cases. Furthermore, under the assumption of the factorization we try to calculate the structure function of the exotic component $F^2_{exo}(x)$ by employing their dynamical rescaling hypothesis. However we find this trial cannot succeed in reproducing the experimental data with our values of $P^2_{exo}(A)$. Further study especially on the scaling function $Q(X)$ derived here is now in progress.

Acknowledgement

We thank Prof. M.Muraoka for providing us the clue for the organization of this INS 232, 233 Collaboration. We are grateful to Drs K. Saito and H. Tezuka for their fruitful discussions. One of the author (H.Sumiyoshi) greatly appreciates the financial support by the Faculty of Engineering, Seikei University under the Grant of Special Reserch Project 1984. The numerical calculations have been performed with the FACOM M380R/M380K at INS.

References

1) J.J.Aubert et al., Phys. Lett. 123B (1983) 275.

2) For examples, S.J.Wimpenny, talk given at the 10th Int'l Conf. on Particle and Nuclei, Heidelberg, 1984, (Preprint No. CERN-EP/84-115) and references therein, and K.Rith, talk given at the Int'l Europhysics Conf. on High Energy Physics, Brighton, 1983, (Preprint No. Freiburg Univ. THE?83/5) and references therein.

3) R.G.Arnold et al., Phys. Rev. Lett. 52 (1984) 727.

4) S.Date, K.Saito, H.Sumiyoshi and H.Tezuka, Phys. Rev. Lett. 52 (1984) 2344.

5) M.Oka and K.Yazaki, Prog. Theor. Phys. Vol 66 (1981) 556 and 572.

6) J.M.Greben and A.W.Thomas, Phys. Rev. C30 (1984) 1021.

7) M.Sakai et al., Prog. Theor. Phys. Suppl. No.56 (1974) 32.

8) K.Yoshinada, in Proc. of the Int'l Sympo. on Electromagnetic Properties of Atomic Nuclei, (TIT, Tokyo, 1983) p77 and private communication.

9) M.Glück, E.Hoffmann and E.Reya, Z. Phys. C13 (1982) 119.

10) T.Nakagawa and Y.Oyanagi, "Program System SALS for Nonlinear Least-Squares Fitting in Experimental Science" in Recent Developments in Statistical Inference and Data Analysis, ed. K.Matsushita (North Holland Publishing Company, 1980), p.221.

11) J. Dias de Deus, M.Pimenta and J. Varela, Phys. Rev. D30 (1984) 697.

12) R.L.Jaffe, F.E.Close, R.G.Roberts and G.G.Ross, Phys. Lett. 134B (1984) 449.

Figure Captions

Fig.1 The ratios $R_A(x)$ of the nucleon structure functions for various nuclei. Solid circles are the experimental data[3] without the correction for neutron excess. Solid lines are predicted values with Q(x) extracted from the data[3] and $P^2_{exo}(A)$ calculated with b = 0.55fm.

Fig.2 Probabilities $P_{exo}(A)$ of finding exotic component in various nuclei. Solid circles are $P_{exo}(A)$ extracted from the experimental data[3]. Open marks are caluculated values of $P_{exo}(A)$ based on the picture of two nucleon overlap: Circles obtained with b = 0.5fm, triangles with b = 0.55fm and square with b = 0.6fm.

Table I. Average probabilities $P^2_{exo}(A)$ of the two-body exotic component in nuclei calculated. Values in the parentheses are the sum of the probabilities of the i-body exotic component(i>2).

	$P^2_{exo}(A)$ (%)		
b (fm)	0.5	0.55	0.6
^{4}He	8.36 (0.26)	12.1 (0.58)	15.6 (1.0)
^{9}Be	8.73 (0.38)	11.5 (0.69)	14.2 (1.1)
^{12}C	10.2 (0.55)	13.4 (1.0)	16.4 (1.6)
^{16}O	10.5 (0.61)	13.9 (1.1)	17.0 (1.8)
^{27}Al	12.0 (0.83)	15.8 (1.6)	19.2 (2.5)
^{40}Ca	13.4 (1.1)	17.5 (2.0)	21.2 (3.3)
^{56}Fe	14.1 (1.2)	18.4 (2.3)	22.2 (3.7)
^{64}Cu	15.6 (1.5)	19.6 (2.6)	23.7 (4.3)
^{90}Zr	15.2 (1.5)	19.7 (2.9)	23.6 (4.4)
^{108}Ag	14.9 (1.4)	19.4 (2.6)	23.3 (4.3)
Sn	15.2 (1.5)	19.3 (2.6)	23.4 (4.2)
^{197}Au	14.8 (1.4)	19.4 (2.6)	23.7 (4.3)
^{208}Pb	14.6 (1.3)	20.0 (2.8)	24.1 (4.7)

Table II. Probability $P^{2,\alpha}_{exo}(A)$ of the two-body exotic component for the nucleon at the particular single particle state in ^{40}Ca.

	$P^{2,\alpha}_{exo}(A)$ (%)
$0s_{1/2}$	21.6
$0p_{3/2}$	18.8
$0p_{1/2}$	19.1
$0d_{5/2}$	15.6
$1s_{1/2}$	16.0
$0d_{3/2}$	16.0

Table III. Probabilities $P_{exo}(A)$ of the exotic component in nuclei, which are determined so as to fit the experimental $R_A(x)$.

	$P_{exo}(A)$ (%)
^{8}Be	10 ± 1
^{9}Be	10 ± 1
^{12}C	14.5 ± 1.3
^{27}Al	15.8
^{40}Ca	19.6 ± 1.5
^{56}Fe	19.5 ± 1.3
^{108}Ag	19.5 ± 1.6
^{197}Au	24.4 ± 1.8

Table IV. Co-efficients of the function $Q(x)=\sum_{l=0}^{4} c_l x^l$.

l	c_l
0	9.29
1	-69.81
2	216.47
3	-248.56
4	150.57

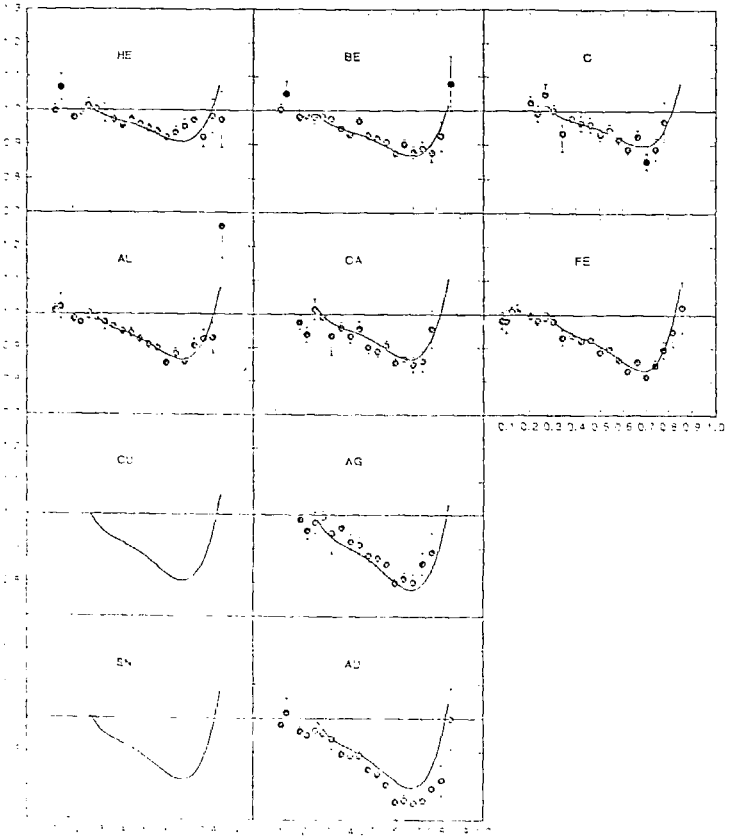

Fig.1

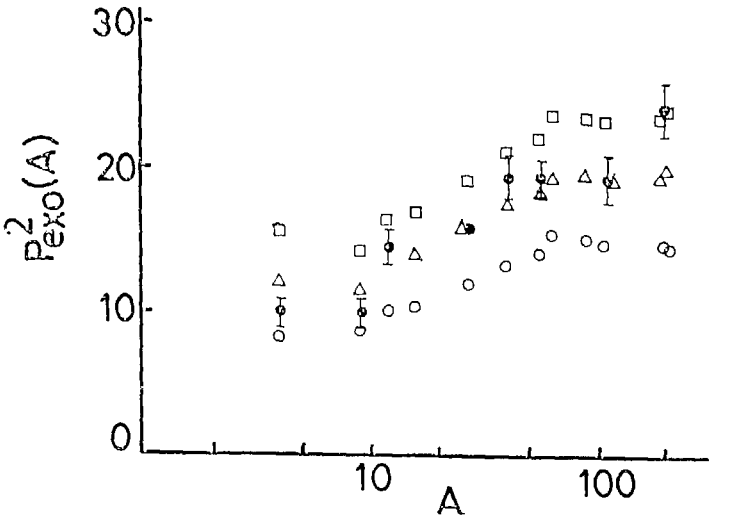

Fig.2